

ARTICLE

Influence of trifocal intraocular lenses on standard autorefractometry and aberrometer-based autorefractometry

 Nuria Garzón, PhD,  María García-Montero, PhD,  Esther López-Artero, MSc,  Francisco Poyales, MD,  César Albarrán-Diego, PhD

Purpose: To study the agreement between manifest refraction and objective refraction measured with two autorefractor models and an aberrometer in eyes implanted with a trifocal diffractive intraocular lens (IOL).

Setting: IOA Madrid Innova Ocular, Madrid, Spain.

Design: Prospective comparative cohort study.

Methods: An autorefractor keratometer (KR-8800), based on a Scheiner double pinhole, and a 3-dimension wavefront topography aberrometer system (OPD-Scan III), based on the scanning-slit retinoscopy principle, were used to obtain objective refraction readings. In addition, lower-order Zernike coefficients (Z) were used to calculate objective refraction. A set of 7 different results was obtained in power vector notation (spherical equivalent [SE], Jackson cross-cylinder, axes at 180 degrees and 90 degrees [J0] and Jackson cross-cylinder, axes at 45 degrees and 135 degrees [J45]) for 7 different methods: manifest refraction, autorefractometry obtained with the autorefractor keratometer, WF-P (Z-based objective refraction for the photopic pupil), WF-M (Z-based objective refraction for

the mesopic pupil), WF-4 (Z-based objective refraction for a 4.0 mm pupil), OPD-C (autorefractometry measured with the 3-dimension wavefront topography aberrometer system under photopic conditions), and OPD-M (autorefractometry measured with the 3-dimension wavefront topography aberrometer system under mesopic conditions).

Results: The study comprised 102 eyes from 51 cataract patients who underwent binocular implantation of a diffractive trifocal IOL (FineVision POD F). All 6 objective methods yielded more negative SE values than manifest refraction ($P < .001$). As for the astigmatism components (J0 and J45), only autorefractometry ($P = .003$) and OPD-M ($P < .001$) differed significantly from manifest refraction. The best and worst correlation for the SE component were intraclass correlation coefficient (ICC) = 0.70 (for WF-M) and ICC = 0.48 (for WF-4).

Conclusion: Objective methods tend to yield more negative sphere values than manifest refraction.

J Cataract Refract Surg 2019; ■:■-■ © 2019 ASCRS and ESCRS

Cataract surgery is increasingly becoming a refractive surgery procedure that seeks to provide patients with the best possible vision for all viewing distances. Multifocal intraocular lens (IOL) implantation enables the patient to be spectacle-free after cataract surgery for both distance and near vision, offering an improved quality of life; therefore, the number of patients opting for this type of IOL has increased. These IOLs can be classified based on their design: namely, there are refractive versus diffractive; monofocal, bifocal, or trifocal; and they can be either rotationally symmetric or asymmetric.

Multifocal IOLs make the most of the brain's ability to adapt to far or near vision because different elements of

the lens are used, depending on where the patient is focusing.

In devising the present study, our main goal was to assess the quality of vision that multifocal IOLs provide using both the standard approach and quicker alternative measuring techniques. Subjective or manifest refraction is the gold-standard method to determine the eye's refractive status, whereas autorefractometry is considered a fast and reliable method to measure refraction in the general population. However, autorefractometry has not yet been able to fully oust and replace manifest refraction; in fact, it is commonly used just to provide an optimum starting point for manifest refraction assessment. The accuracy of autorefractometry can

Submitted: December 28, 2018 | Final revision submitted: April 16, 2019 | Accepted: April 17, 2019

From the IOA Madrid Innova Ocular (Garzón, López-Artero, Poyales), Madrid, Optometry and Vision Department (Garzón, García-Montero), Faculty of Optics and Optometry, Complutense University of Madrid, Optics (Albarrán-Diego), Optometry and Vision Science Department, Faculty of Physics, University of Valencia, and Clínica Baviera Castellón (Albarrán-Diego), Castellón de la Plana, Spain.

Corresponding author: Nuria Garzón, PhD, IOA Madrid Innova Ocular, C/Galileo 104, 28003 Madrid, Spain. E-mail: ngarzon@ioamadrid.com.

be compromised by previous corneal refractive surgeries, media opacities, a small pupil size, and the presence of multifocal IOLs.^{1–5}

In this context, the purpose of this study was to evaluate the agreement between manifest refraction and the objective refraction readings provided by the aforementioned automated devices in eyes that had diffractive trifocal IOL implantation.

MATERIALS AND METHODS

Study Design and Patient Population

This was a prospective comparative cohort study of patients undergoing cataract surgery and binocular implantation of a trifocal IOL (FineVision POD F, PhysiOL S.A.) at IOA Madrid Innova Ocular, Madrid, Spain. All patients provided written informed consent before enrollment. This study was approved by the local ethics committee, and it was performed in accordance with the Declaration of Helsinki.

Other inclusion criteria were the desire for spectacle independence after surgery with realistic expectations and the availability and willingness to comply with all the study visits and eye examinations.

Exclusion criteria were a history of ocular disease other than cataract (eg, uveitis, amblyopia, glaucoma), astigmatism above 1.25 diopters (D), any acute or chronic condition that would increase the risk or confound study results, any capsule or zonular abnormalities that might affect postoperative centration or tilt of the IOL, and the presence of pupil abnormalities.

Surgical Procedure

All surgeries were carried out by the same surgeon (F.P.) under topical anesthesia. A 2.2 mm corneal incision and a paracentesis were made with a surgical knife. Anterior capsulotomy and nuclear fragmentation were performed with a femtosecond laser under optical coherence tomography image control (CATALYS Precision System, Abbott Medical Optics, Inc.), and for lens phacoemulsification, a commercial microsurgical system (Centurion Vision System, Alcon Laboratories, Inc.) was employed. Two ophthalmic viscosurgical devices were used throughout the entire procedure: the cohesive sodium hyaluronate 1.0% (Healon) and the dispersive sodium hyaluronate 1.2% (Amvisc). The POD F IOL was then implanted into the capsular bag with a single-use injection system (Microse, PhysiOL S.A.). In all cases, a capsular tension ring was inserted. All surgeries were supported by the computer-assisted cataract surgery system (CALLISTO Eye from the Cataract Suite Markerless, Carl Zeiss Meditec AG).

Once the procedure was completed, patients were treated with a combination of antibiotics, corticosteroids, and antiinflammatory eye drops (moxifloxacin, dexamethasone, and bromfenac).

Intraocular Lens

The POD F IOL model is a spherical trifocal IOL that combines two diffractive structures. This combination provides three foci: +0.00 D for far vision, a +1.75 D addition for intermediate vision, and a +3.50 D addition for near vision. This corresponds to a nominal intermediate addition of approximately +1.2 D and a near addition of approximately +2.4 D at the corneal plane, depending on the particular geometry of the eye. The IOL's optics is biconvex aspheric (spherical aberration [SA] $-0.11 \mu\text{m}$). The IOL has a diffractive anterior surface that is entirely convoluted. By varying the step height of the IOL's diffractive structure across the pupil, the energy distribution for different distances can be controlled.⁶ The amount of energy directed to far vision focus is superior to that directed to intermediate and near vision focus with increasing apertures by a gradual decrease in the height of diffractive steps from the center to the periphery, which is also the

case for the refractive multifocal IOL. The lens is 26% hydrophilic acrylic and has a ultraviolet and blue-light blocker. It has an optic-body diameter of 6.00 mm and an overall diameter of 11.40 mm, its refractive index is 1.46, and it has a 5-degree angulation.

Postoperative Eye Examinations

Subjective Refraction Patients were examined 1 day, 1 week, and 1 month after surgery, although the data reported in this paper were taken at the 1-month visit. The decision to analyze the 1-month postoperative data was based on the study authors' previous experience regarding the stability of refractive results at this time, and not before.

All refraction assessments were carried out by the same optometrist (N.G.). Manifest refraction was always performed under photopic conditions, with the same illumination for all patients, using the Early Treatment Diabetic Retinopathy Study chart with a trial frame. Objective refraction was measured under both photopic and mesopic conditions. The best visual acuity scenario manifest refraction was then further fine-tuned—both spherical and cylindrical components—with cross-cylinders in steps of 0.25 D. Other tests that were performed were biomicroscopy, tonometry, and fundus evaluation.

Autorefractometry The autorefractor keratometer (KR-8800, Topcon Corp.) is a multifunctional device that determines corneal refractive status using a rotary prism measuring system. This device provides keratometry measurements for corneal diameters ranging from 2.0 mm to 7.7 mm according to the presence of anterior corneal astigmatism, with keratometry values and corneal curvatures obtained over a range from 5.00 mm to 10.00 mm (0.01 mm, step display). The autorefractor keratometer relies on the Scheiner double-pinhole principle for data capture: two light sources are imaged onto the pupil plane to simulate the Scheiner pinhole apertures. First, the Badal system is focused onto one meridian, and then continuous measurements are taken throughout a 180-degree range using a rotating prism system. A “fogging” target was used to relax accommodation.⁷ Automatic capture of 4 measures was repeated twice, and the average values were used for statistical analysis. Measurement accuracy was set to 0.12 D for power and to 1 degree for axis, as advised by the manufacturer.^{8,9}

Aberrometry The 3-dimension wavefront topography aberrometer system (OPD-Scan III, Nidek Co., Ltd.) is an aberrometer–corneal topographer workstation. It combines a wavefront aberrometer, a topographer, an autorefractor, an autokeratometer, and a pupillometer, all in one device. The autorefractor relies on the principle of scanning-slit retinoscopy, where the retina is scanned with an infrared slit beam. Measurement light emitted in a grid-like pattern is projected onto the retina, and the light reflected from the retina is then captured by multiple pairs of photodetectors. Refraction of the eye causes time (phase) differences in the signals sent out by these pairs of photodetectors. The device calculates the patient's refraction (spherical and cylindrical refractive errors, as well as the cylinder axes angle) based on these phase differences.¹⁰ In addition to providing objective refraction in the form of a spherocylindrical reading, the aberrometer also computes the Zernike coefficients for lower-order and higher-order aberrations. The Zernike coefficients corresponding to lower-order aberrations $Z(0,2)$, $Z(2,+2)$ and $Z(2,-2)$ can be used to calculate objective refraction in vector notation (SE, J0, and J45) according to the following expressions¹¹:

$$SE = \frac{4\sqrt{3}}{r^2} Z_2^0$$

$$J_0 = \frac{2\sqrt{6}}{r^2} Z_2^{+2}$$

$$J_{45} = \frac{2\sqrt{6}}{r^2} Z_2^{-2}$$

where r is the pupil radius (or semidiameter) measured by the 3-dimension wavefront topography aberrometer system either in photopic or mesopic conditions, SE is the spherical equivalent, J0 is the vertical Jackson cross-cylinder, axes at 180 degrees and 90 degrees and J45 is the oblique Jackson cross-cylinder, axes at 45 degrees and 135 degrees.

Moreover, these vector components can be turned into the more common clinical spherocylindrical notation (sphere [S], cylinder [C], and axis [A]) using the following expressions^{11,12}:

$$C = -2\sqrt{J_0^2 + J_{45}^2}$$

$$S = SE - \frac{C}{2}$$

$$A = \frac{1}{2} \tan^{-1} \frac{J_{45}}{J_0}$$

Statistical Analysis

The manifest refraction and objective refraction values obtained in clinical spherocylindrical notation were converted into power-vector notation for comparison purposes, by means of the following expressions¹¹:

$$SE = S + \frac{C}{2}$$

$$J_0 = -\frac{C}{2} \cos 2A$$

$$J_{45} = -\frac{C}{2} \sin 2A$$

A set of three objective refraction calculations of the Zernike coefficients were performed: one for photopic pupil, one for mesopic pupil, and one for a "standard" pupil fixed at 4.0 mm because this was the value yielding the best agreement for SE in a previous study by Campbell.¹³ Given that the IOL implanted in this study has an aspherical profile (SA = -0.11 μ m) not designed to fully compensate for the average corneal SA of the human eye (~0.27 μ m), a decision was made to consider automated objective refraction values for more than one pupil diameter to check whether one of those objective measurements was statistically better correlated to subjective refraction than the others.

For each eye included in the study, 7 result sets (one for each assessment method) were collected: manifest refraction, autorefractometer measured with the autorefractor keratometer, WF-P (Zernike-coefficients-based objective refraction, photopic pupil size), WF-M (Zernike-coefficients-based objective refraction, mesopic pupil size), WF-4 (Zernike-coefficients-based objective refraction, 4.0 mm pupil), OPD-C (autorefractometer measured with the 3-dimension wavefront topography aberrometer system in the central pupil/photopic conditions), and OPD-M (autorefractometer measured with the 3-dimension wavefront topography aberrometer system under mesopic conditions).

SigmaPlot software for Windows (version 12, Systat Software, Inc.) was used for statistical analysis and graphic plotting. The Friedman repeated-measurements analysis of variance on ranks was used to look for differences across the 7 assessment methods for each of the refraction vector components. When differences were found, pairwise multiple-comparison testing was applied by the Tukey test to identify those differences. Agreement was evaluated with Bland-Altman plots, and ICCs were calculated with Medcalc Statistical software for Windows (version 12.5, MedCalc Software bvba) to study the strength

Table 1. Descriptive statistics obtained after surgery for refraction and visual acuity.

Parameter	Mean \pm SD	Range
Refraction (D)		
SE	-0.08 \pm 0.27	-1.00, 0.50
J0	-0.03 \pm 0.13	-0.48, 0.25
J45	0.01 \pm 0.11	-0.35, 0.43
Sph	0.01 \pm 0.25	-0.75, 0.75
Cyl	-0.17 \pm 0.31	-1.25, 0.00
Visual acuity (logMAR)		
UDVA	0.04 \pm 0.07	0.40, -0.10
CDVA	0.00 \pm 0.03	0.14, -0.10

CDVA = corrected distance visual acuity; Cyl = cylinder; J0 = vertical Jackson cross-cylinder, axes at 180 degrees and 90 degrees; J45 = oblique Jackson cross-cylinder, axes at 45 degrees and 135 degrees; logMAR = logarithm of the minimum angle of resolution; SE = spherical equivalent; Sph = sphere; UDVA = uncorrected distance visual acuity

of the agreement between methods.¹⁴ Statistical significance was set at $\alpha = 0.05$.

Considering a repeated-measurements design, with 0.25 diopters (D) as the minimum clinically relevant difference in refraction, and estimating an expected standard deviation of the differences two times this mean value (0.50 D, based on previous exploratory measurements), the sample size estimated with the SigmaPlot software to reach a proper statistical power ($1 - \beta$) = 0.80, resulted in $n = 34$. A decision was then made to recruit as many patients as possible above this amount.

RESULTS

The study comprised 102 eyes from 51 patients. The mean age was 67.2 years \pm 8.5 (SD). The mean pupil size was 3.31 \pm 0.62 mm and 4.71 \pm 0.84 mm under photopic and mesopic conditions, respectively.

Table 1 shows a summary of the surgical outcomes in terms of refraction and visual acuity. The average refractive result was very close to emmetropia, with a mean SE of -0.08 D and both astigmatic components being below 0.05 D.

Figure 1 shows a boxplot illustrating the differences between manifest refraction outcomes and each of the 6 objective refraction measuring approaches under evaluation, for sphere, SE, and the astigmatism components (J0 and J45).

Table 2 shows means \pm SD and range for all the objective refraction methods considered.

As Figure 1 shows, all 6 objective methods produced more negative—or less positive—sphere and SE outcomes than manifest (subjective) refraction. In particular, WF-P yielded the biggest average difference for SE (mean difference with manifest refraction: -0.73 \pm 0.69 D), whereas the closest results to manifest refraction were obtained with OPD-C (mean difference with manifest refraction: -0.27 \pm 0.34 D). Regarding the astigmatism components, for J0, WF-M was closest to the manifest refraction readings (mean difference: 0.00 \pm 0.20 D), whereas autorefractometer yielded the biggest—although minor—differences with manifest refraction (mean difference: -0.07 \pm 0.19 D). In contrast, for the J45 component, the lowest differences were obtained with autorefractometer (0.01 \pm 0.14 D), whereas

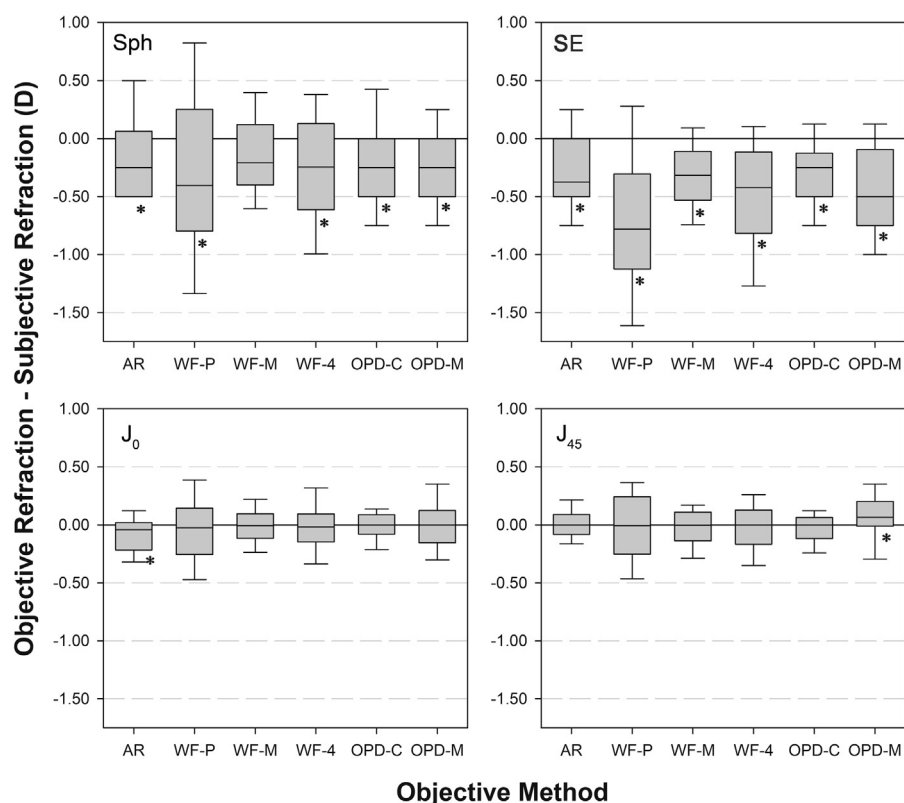


Figure 1. Differences between objective refraction and subjective (manifest) refraction for sphere, SE, and J₀ and J₄₅ (vector components of astigmatism), and for each of the 6 objective refraction scenarios under assessment. The asterisks (*) indicate statistically significant differences (AR = autorefractometer; J₀ = vertical Jackson cross-cylinder, axes at 180 degrees and 90 degrees; J₄₅ = oblique Jackson cross-cylinder, axes at 45 degrees and 135 degrees; OPD-C = autorefractometer measured with the 3-dimension wavefront topography aberrometer system in the central pupil/photopic conditions; OPD-M = autorefractometer measured with the 3-dimension wavefront topography aberrometer system under mesopic conditions; SE = spherical equivalent; Sph = sphere; WF-4 = wavefront 4.0 mm; WF-M = wavefront mesopic; WF-P = wavefront photopic).

OPD-M yielded the largest differences with manifest refraction (0.06 ± 0.24 D).

Using the Friedman repeated-measures analysis of variance on ranks, statistically significant differences were found between manifest refraction and the objective refraction approaches, both for the sphere ($P < .001$) and SE ($P < .001$) values. In particular, the post hoc testing for sphere revealed differences between manifest refraction and each of the objective methods, except for WF-M. As for SE, the Turkey post hoc testing revealed differences between manifest refraction and each of the objective methods. Regarding astigmatism, the Friedman repeated-measures analysis of variance on ranks also revealed statistically significant differences between methods, both for J₀ ($P = .003$) and J₄₅ ($P < .001$). More specifically, post hoc testing identified significant differences for J₀ only between manifest refraction and autorefractometer (but not for the remaining manifest refraction-objective refraction pairwise comparison), whereas for J₄₅, it was manifest refraction versus OPD-M, which was the only pairwise comparison that yielded significant differences from the 6 objective refraction approaches.

Figures 2 through 5 show the Bland-Altman plots for sphere and each component of the power vector. In each plot, the vertical axis represents the difference found between each objective method and the subjective manifest refraction outcomes, whereas the horizontal axis indicates the corresponding manifest refraction value. This absolute manifest refraction value was plotted, rather than plotting the average across all methods, because subjective refraction is considered the gold standard technique for refractive status determination.

Table 3 shows the resulting ICCs for each measuring method and for each refractive component. The strongest correlation with manifest refraction for sphere values was found for WF-M, whereas the weakest was for WF-P. For the SE, the strongest and weakest correlations with manifest refraction were for WF-M and WF-4, respectively. Autorefractometer showed the strongest correlation with manifest refraction for astigmatism, whereas WF-P showed the weakest correlation.

DISCUSSION

This prospective study compared clinically obtained manifest refraction versus objective refraction after trifocal diffractive IOL implantation.

Because of the multifocal nature of trifocal diffractive IOLs, their depth of focus is larger than that of standard monofocal IOLs. The absence of a unique focal plane makes it more difficult for us to determine unambiguously and accurately our patients' objective or subjective manifest refraction.¹⁵

Several methods are available to estimate refractive error after lens extraction and IOL implantation; these include keratometry, retinoscopy, and autorefractometer; however, manifest refraction is still considered the gold standard. Autorefractometer's accuracy has been found to decrease in the presence of a multifocal IOL,^{2,4,16} whereas retinoscopy becomes more complicated to perform with some of these lenses—such as refractive sectorial IOLs—because of the presence of two opposite retinoscopy shadows.¹

Several authors have compared objective and subjective refraction values in refractive and bifocal diffractive IOL

Table 2. Descriptive statistics for the objective refractions obtained with all the evaluated methods.

Parameter	AR	WF-P	WF-M	WF-4	OPD-C	OPD-M
Sph						
Mean \pm SD	-0.13 ± 0.41	-0.30 ± 0.87	-0.15 ± 0.43	-0.25 ± 0.62	-0.17 ± 0.44	-0.25 ± 0.43
Range	-0.75, 1.00	-2.85, 2.52	-1.50, 1.12	-1.86, 1.49	-1.50, 1.25	-1.75, 0.50
Cyl						
Mean \pm SD	-0.48 ± 0.35	-1.00 ± 0.66	-0.48 ± 0.30	-0.66 ± 0.42	-0.35 ± 0.31	-0.50 ± 0.58
Range	-1.50, 0.00	-3.47, -0.03	-1.54, -0.02	-1.98, -0.02	-1.50, 0.00	-2.25, 1.50
SE						
Mean \pm SD	-0.37 ± 0.40	-0.80 ± 0.80	-0.39 ± 0.39	-0.58 ± 0.60	-0.35 ± 0.41	-0.50 ± 0.51
Range	-1.13, 0.88	-2.87, 1.10	-1.51, 0.57	-2.18, 1.07	-1.50, 0.63	-1.88, 0.88
J0						
Mean \pm SD	-0.11 ± 0.22	-0.08 ± 0.46	-0.04 ± 0.22	-0.05 ± 0.29	-0.04 ± 0.17	-0.01 ± 0.29
Range	-0.73, 0.37	-1.70, 1.18	-0.76, 0.58	-0.82, 0.77	-0.74, 0.49	-0.74, 1.12
J45						
Mean \pm SD	0.02 ± 0.17	-0.02 ± 0.38	-0.01 ± 0.18	-0.02 ± 0.26	-0.02 ± 0.15	0.07 ± 0.24
Range	-0.38, 0.65	-1.21, 0.97	-0.54, 0.44	-0.93, 0.55	-0.61, 0.37	-0.86, 0.79

AR = autorefraction; Cyl = cylinder; J0 = vertical Jackson cross-cylinder, axes at 180 degrees and 90 degrees; J45 = oblique Jackson cross-cylinder, axes at 45 degrees and 135 degrees; OPD-C = autorefraction measured with the 3-dimension wavefront topography aberrometer system in the central pupil/photopic conditions; OPD-M = autorefraction measured with the 3-dimension wavefront topography aberrometer system under mesopic conditions; SE = spherical equivalent; Sph = sphere; WF-4 = wavefront 4.0 mm; WF-M = wavefront mesopic; WF-P = wavefront photopic

wearers; however, to our knowledge, this is the first attempt to perform such a comparison with the more complex trifocal IOLs, which have three foci (for far, intermediate, and near distances).

Our results suggest that objective methods for postsurgical refraction evaluation (objective refraction) tend to yield more negative sphere values than manifest refraction. A similar tendency has been found for bifocal IOLs to a

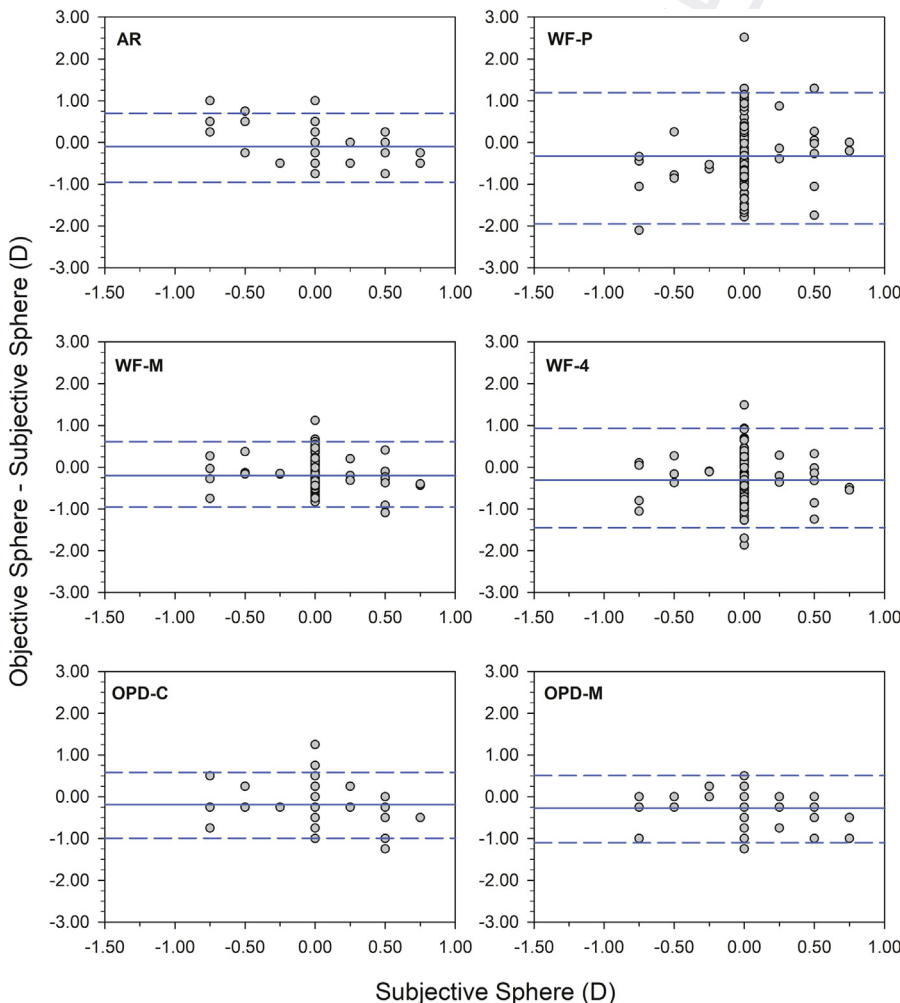


Figure 2. Bland-Altman plots for the sphere, showing the agreement between subjective (manifest) refraction and each of the 6 objective refraction approaches (AR = autorefraction; OPD-C = autorefraction measured with the 3-dimension wavefront topography aberrometer system in the central pupil/photopic conditions; OPD-M = autorefraction measured with the 3-dimension wavefront topography aberrometer system under mesopic conditions; WF-4 = wavefront 4.0 mm; WF-M = wavefront mesopic; WF-P = wavefront photopic).

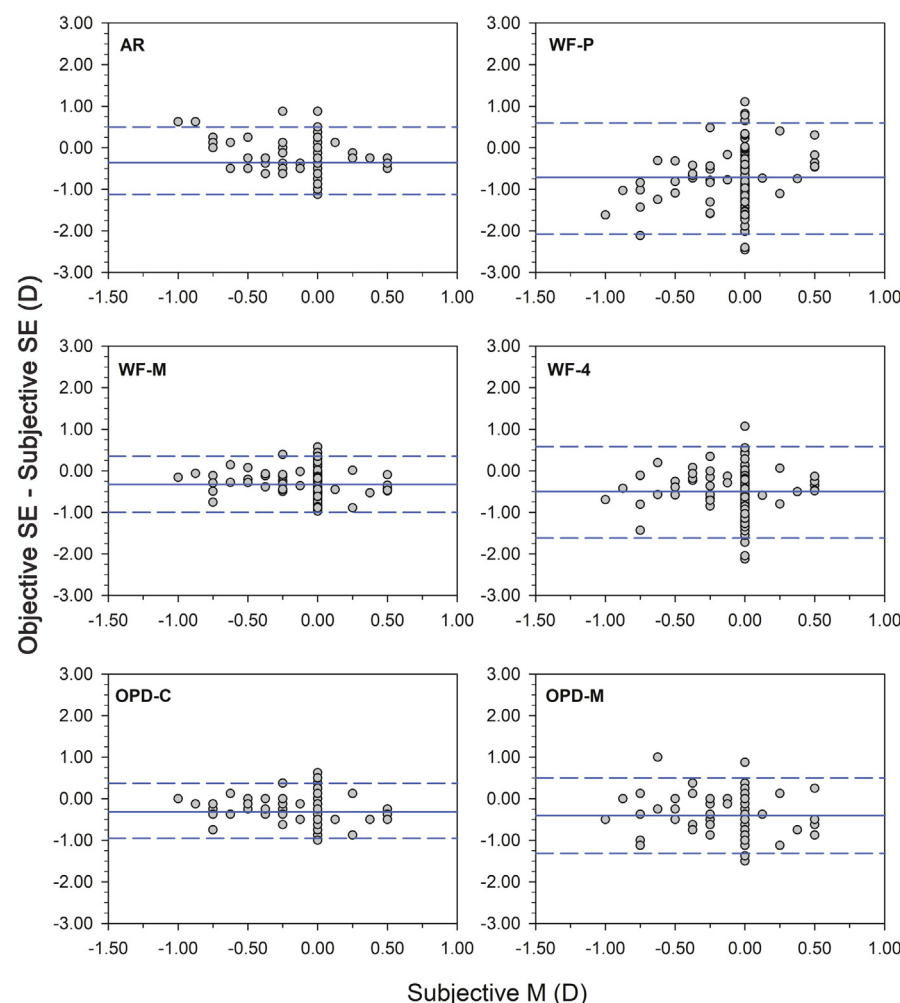


Figure 3. Bland-Altman plots for SE, showing the agreement between subjective (manifest) refraction and each of the 6 objective refraction approaches (AR = autorefraction; OPD-C = autorefraction measured with the 3-dimension wavefront topography aberrometer system in the central pupil/photopic conditions; OPD-M = autorefraction measured with the 3-dimension wavefront topography aberrometer system under mesopic conditions; SE = spherical equivalent; WF-4 = wavefront 4.0 mm; WF-M = wavefront mesopic; WF-P = wavefront photopic).

greater or lesser extent and, more specifically, a stronger trend toward myopia has been observed for refractive bifocal IOLs than for diffractive ones.^{4,17}

As for sectorial refractive IOLs, van der Linden et al.² and Albarrán-Diego et al.¹ found a systematic shift toward more negative values for autorefraction, between 1.00 D and 1.25 D, compared with subjective refraction, with poor correlation for cylinder values. Bissen-Miyajima et al.³ reported similar issues with refractive IOLs, hypothesizing that pupil size might confound autorefraction outcomes; actually, the geometry of the lens could be the main factor causing measurement inaccuracy.

Other studies, which compared a concentric refractive IOL model with two bifocal diffractive ones,^{4,17} concluded that the presence in the IOL of several concentric refractive zones—which results in the overlapping of two images at the retinal plane—could cause an undesirable scattering of the autorefractor's infrared beam, thus leading to inaccurate results.

In contrast, with diffractive bifocal IOL wearers, the autorefractor proved useful as a starting point to estimate manifest refraction—both its spherical and its astigmatic components—thus highlighting the noteworthy differences between refractive and diffractive IOLs.⁴ In their study, Muñoz et al.⁴ found that the

mean spherical power difference between autorefraction and subjective refraction was near zero for the bifocal diffractive IOL models considered (0.03 ± 0.09 D for the Restor model [Alcon Laboratories, Inc.] and -0.05 ± 0.11 D for the Tecnis model [Johnson & Johnson Vision Care, Inc.]).

As for our study, encompassing trifocal diffractive IOL wearers only, we assessed two autorefractor models—one that was based on the Scheiner double-pinhole principle (autorefractor keratometer) for data capture and another one that relies on the principle of scanning-slit retinoscopy (3-dimension wavefront topography system, used under either photopic or mesopic conditions)—together with an aberrometer that can measure the aberration pattern for different pupil sizes. Similar results were obtained for the autorefractor keratometer (mean difference between objective refraction and manifest refraction: -0.29 ± 0.39 D) and the 3-dimension wavefront topography aberrometer system under photopic conditions (mean difference between objective refraction and manifest refraction: -0.27 ± 0.34 D). The results did not correlate as well when using the 3-dimension wavefront topography aberrometer system under mesopic conditions (mean difference between objective refraction and manifest refraction: -0.42 ± 0.47 D).

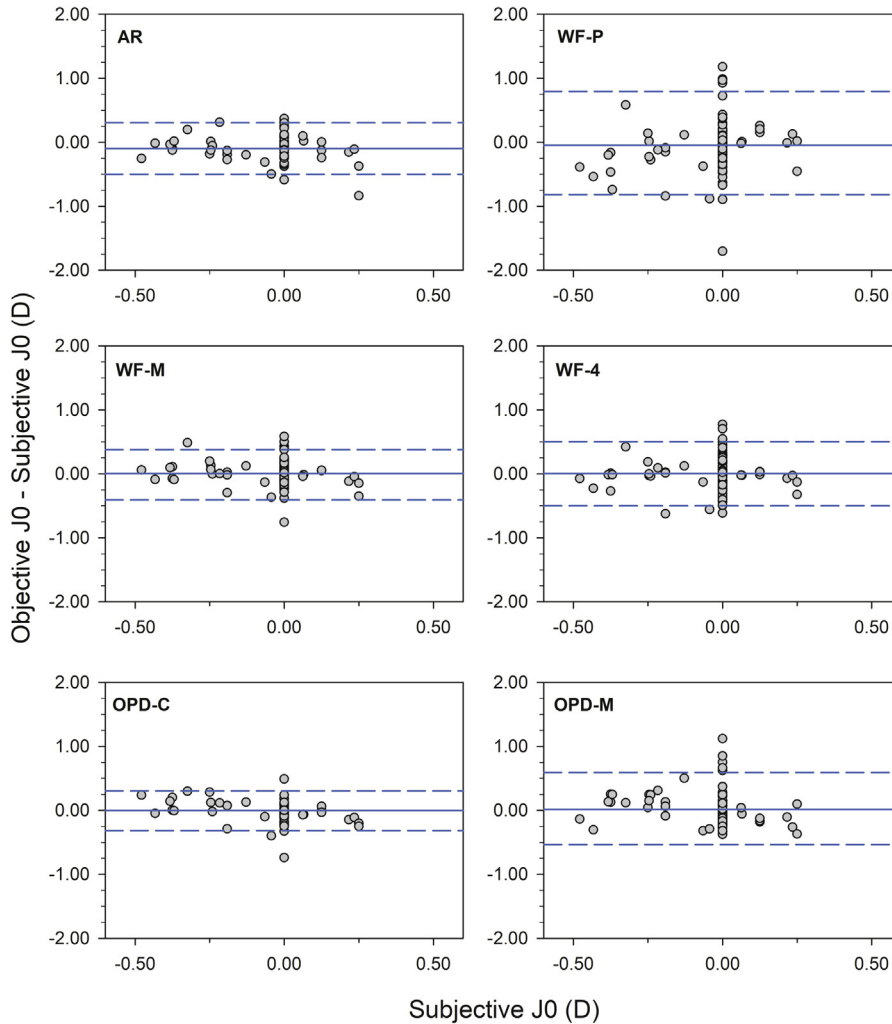


Figure 4. Bland-Altman plots for J0 (vector component of astigmatism), showing the agreement between subjective (manifest) refraction and each of the 6 objective refraction methods (AR = autorefraction; J0 = vertical Jackson cross-cylinder, axes at 180 degrees and 90 degrees; OPD-C = autorefraction measured with the 3-dimension wavefront topography aberrometer system in the central pupil/photopic conditions; OPD-M = autorefraction measured with the 3-dimension wavefront topography aberrometer system under mesopic conditions; WF-4 = wavefront 4.0 mm; WF-M = wavefront mesopic; WF-P = wavefront photopic).

In our study we found a more myopic shift in objective refraction values with trifocal IOLs than that found in the studies by Muñoz et al.^{4,17} with bifocal IOLs. The addition of a third focus could be one of the reasons, but pupil size and SA could also be a couple of factors explaining this behaviour. In our sample, the mean value for spherical power in subjective refraction was near zero (-0.08 ± 0.27), whereas objective measurements yielded average values ranging from -0.13 ± 0.41 (for autorefraction) to -0.30 ± 0.87 (for the WF-P). The implanted lens has an SA of $-0.11 \mu\text{m}$, which is not enough to compensate for the average corneal SA. In fact, total SA in our cohort post-operatively, resulted in a mean value of $0.24 \pm 0.13 \mu\text{m}$. This could explain why 3-dimension wavefront topography aberrometer system measurements resulted in more myopic objective refractions for mesopic than photopic pupil. Also, this could explain the myopic shift when compared with subjective refraction, in which the Stiles Crawford effect could account for the bigger height of the central than the peripheral rays incoming the pupil, and thus, diluting the effect of SA.

Concerning the use of aberrometry to assess multifocal IOL wearers, Charman et al.¹⁸ concluded that a Hartmann-Shack aberrometer might not provide reliable

information on the wavefront aberration associated with either the distance or the near components of diffractive IOLs because the results could depend on factors such as the power of the diffractive addition and the relative amplitudes of the distance and near wavefronts.

In this same context, Campbell¹⁹ used a Hartmann-Shack WaveScan aberrometer (Abbott Medical Optics, Inc.) to evaluate two different IOLs: a refractive model (ReZoom, Abbott Medical Optics, Inc.) versus a diffractive one (Tecnis multifocal +4.00). The study was performed in an artificial eye, and in this scenario, he was not able to reliably measure distance refraction and higher-order aberrations with a clear tendency toward myopia (the sphere was higher than -1.25 D , and it was dependent on pupil size). In contrast, the Tecnis IOL could be measured reliably; the values obtained were close to the set value of 0.00 D of sphere.

Jendritza et al.²⁰ found a similar trend in vivo for a diffractive IOL (Tecnis multifocal +4.00) when using the same aberrometer as Campbell¹⁹ to compare its readings with manifest refraction values (sphere +0.45D, cylinder -0.14 D). When assessing wearers of a diffractive apodized IOL (Restor +4.00), aberrometer results and manifest refraction values were very comparable; however, the

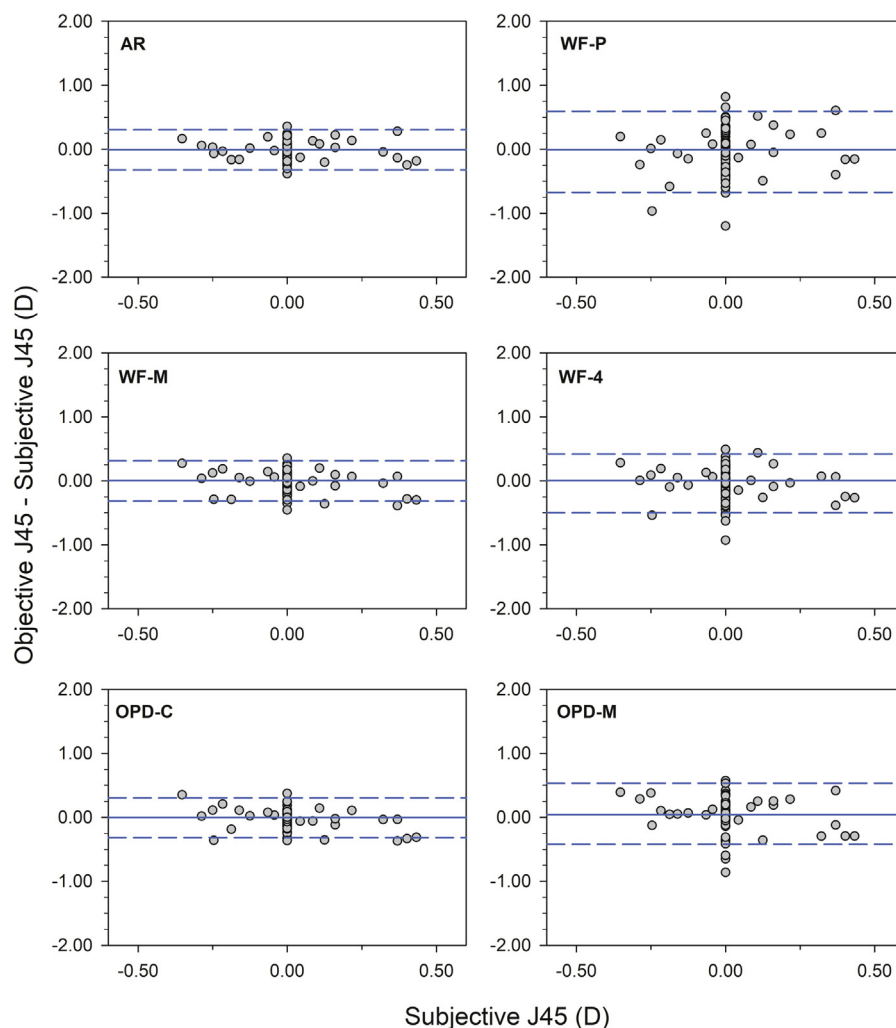


Figure 5. Bland-Altman plots for J45 (vector component of astigmatism), showing the agreement between subjective (manifest) refraction and each of the 6 objective refraction approaches (AR = autorefractometry; J45 = oblique Jackson cross-cylinder, axes at 45 degrees and 135 degrees; OPD-C = autorefractometry measured with the 3-dimension wavefront topography aberrometer system in the central pupil/photopic conditions; OPD-M = autorefractometry measured with the 3-dimension wavefront topography aberrometer system under mesopic conditions; WF-4 = wavefront 4.0 mm; WF-M = wavefront mesopic; WF-P = wavefront photopic).

former showed greater variability than the latter and tendency toward myopia (sphere -0.34 D, cylinder -0.20 D). Our findings, which also reveal a slight trend toward myopia, are in good agreement with these studies.

As for our assessment of the 3-dimension wavefront topography aberrometer system, which is based on the scanning-slit retinoscopy principle, it is worth highlighting that the SE readings that were closest to manifest refraction were obtained with this aberrometer under mesopic conditions (-0.32 ± 0.32 D), whereas the readings that differed the most were the ones yielded by this same aberrometer

but under photopic conditions (-0.73 ± 0.69 D). Compared with the Jendritza et al.²⁰ results for a 4.0 mm pupil, our results showed more myopia drift (sphere -0.26 D versus $+0.45$ D respectively).

Regarding the astigmatic components of the power vector, the resulting J0 and J45 were similar for the aberrometers—close to 0.00 D—irrespective of pupil size. We would like to emphasize the importance of understanding the distinction between “statistical” and “clinical” differences. These astigmatic components showed very low values in our patient population

Table 3. ICCs for each of the methods and for each of the refractive components.

Parameter	ICC					
	AR	WF-P	WF-M	WF-4	OPD-C	OPD-M
Sph	0.45	0.38	0.57	0.43	0.52	0.49
SE	0.51	0.50	0.70	0.48	0.69	0.52
J0	0.60	0.39	0.58	0.49	0.62	0.40
J45	0.72	0.37	0.56	0.41	0.58	0.37

AR = autorefractometry; ICC = intraclass correlation coefficient; J0 = vertical Jackson cross-cylinder, axes at 180 degrees and 90 degrees; J45 = oblique Jackson cross-cylinder, axes at 45 degrees and 135 degrees; OPD-C = autorefractometry measured with the 3-dimension wavefront topography aberrometer system in the central pupil/photopic conditions; OPD-M = autorefractometry measured with the 3-dimension wavefront topography aberrometer system under mesopic conditions; SE = spherical equivalent; Sph = sphere; WF-4 = wavefront 4.0 mm; WF-M = wavefront mesopic; WF-P = wavefront photopic

(resulting from the low-astigmatism inclusion criterion); therefore, even though statistical testing did reveal significant differences (see autorefraction for J0 and OPD-M for J45 in Figure 1), those differences are not clinically relevant because the magnitude was below 0.1 D (see Table 2).

It is well known that diffractive efficiency falls and add power increases as wavelength increases^{21,22}; therefore, it might be that the Hartmann-Shack aberrometers that use longer infrared-light wavelengths are more likely to produce wavefront results that correspond to the wavefront produced by the distance power of a diffractive IOL. This problem should not arise when using the OPD-Scan III aberrometer because it relies on a different principle (ie, retinoscopy); however, as mentioned above, relevant differences are observed depending on whether the measurements are performed under either mesopic or photopic conditions.

Discrepancies between objective aberrometer-based refraction and subjective refraction have been attributed to many variables, including the eye's longitudinal chromatic aberration,²³ accommodative status during the objective measurement,²⁴ the different retinal reference planes chosen by each technique,²⁵ the Stiles-Crawford effect,²⁶ image noise in the objective measurements,²⁴ and the merit function that is chosen to determine best focus.²⁷

We hypothesize that the use of narrow beams might lead to erroneous results because the diffractive behavior requires that the area of the lens illuminated is sufficiently large for adequate summation of secondary wavelets to occur.

The sphere component (S) can be calculated in terms of $C(2,0)$, which is the Zernike expansion's defocus coefficient that the aberrometer yields:

$$S = - \left(\frac{4\sqrt{3}c_2^0}{R^2} \right)$$

where R is the pupil radius. Because for a given aberration pattern, the resulting S is inversely proportional to R squared, the impact of defocus will be greater under photopic conditions (ie, small pupil sizes) than under mesopic ones. Moreover, we have to bear in mind that under photopic conditions and when no mydriatic agent has been applied (ie, nondilated pupil), the depth of focus could increase; our hypothesis is that this scenario can make wavefront measurement more difficult, thus resulting in refraction/power calculation errors.

Another parameter that could lead to variability is the wavelength used by the measuring system. It might also contribute to the inaccuracy and imprecision of objective wavefront refraction.²⁸ The optical performance of diffractive multifocal IOLs, measured under either visible or near-infrared illumination differs considerably: namely, these IOLs show two distinct (near and far) foci under visible

light, whereas under near-infrared illumination, their performance outcomes are clearly biased in favor of their far focus. These results might help prevent a misleading use of near-infrared-based clinical instruments for the assessment of eyes implanted with diffractive multifocal IOLs.²⁹ The longer the near-infrared wavelength, the weaker the near focus,^{18,30} and thus, reported wavefront measurements performed with aberrometers that rely on longer wavelengths (808 nm and 850 nm)^{31,32} in patients who have diffractive multifocal IOL implants would produce even more biased results, and the properties of the near focus would be hard to discern because of the much stronger presence of the far focus. The OPD-Scan III uses an 808 nm light source, which could thus lead to the aforementioned measuring errors.

Based on the outcomes of our study about a trifocal IOL, we could conclude that no objective measuring technique is as accurate as the subjective method with which the patient attains the best visual acuity possible. Among the objective methods under assessment, the aberrometer (for mesopic pupil sizes) and the autorefractor keratometer are the ones that achieved the best outcomes.

The results obtained in this work have important implications in those patients with refractive surprise after trifocal IOL implantation programmed for laser enhancement of the residual refraction. The proper measurement of that residual refraction is mandatory to achieve the best result and patient satisfaction. Given that these IOLs have three focus parameters and a greater depth of focus, careful attention must be paid to properly measure the refractive status through the far focus of the IOL, and not through intermediate or near foci. For this reason, a proper starting point for subjective refraction is mandatory, and this point will be achieved properly by taking into account that autorefraction measurements must be reinterpreted by adding nearly 0.25 to 0.50 D to the result. Then refraction can be performed from this starting point, and it should be guided by defocus curve measurement in case of doubt.

Our study has certain limitations that must be taken into consideration: First, the manifest refraction values we have dealt with are close to emmetropia. For surgeries in which a diffractive trifocal IOL is implanted, quality outcomes are measured in terms of postoperative residual refractive error (among other variables); that is why the mean residual cylinder (J0 and J45) and the mean SE were as low as 0.08 D and 0.01 D, respectively. This low-aberration scenario sets important limitations to this type of comparison across measuring techniques (manifest refraction, autorefraction, wavefront, and 3-dimension wavefront topography) to assess the eye's postoperative refractive power.

Additional studies encompassing higher refractive error cases and larger samples covering a wider range of refractive error values would be required to confirm the findings shown in the present paper.

WHAT WAS KNOWN

- Multifocal intraocular lenses (IOLs) can induce errors in objective refraction resulting from their optical design.
- An accurate subjective refraction assessment is mandatory to properly determine the refractive status of an eye implanted with a trifocal IOL.

WHAT THIS PAPER ADDS

- To our knowledge, this was the first comparison of objective and manifest subjective refraction in eyes with trifocal IOLs.
- Aberrometry-based objective refraction assessment was not more accurate than traditional autorefractors in the presence of a trifocal IOL.

REFERENCES

- Albarrán-Diego C, Muñoz G, Rohrweck S, García-Lázaro S, Albero JR. Validity of automated refraction after segmented refractive multifocal intraocular lens implantation. *Int J Ophthalmol* 2017; 10:1728–1733
- van der Linden JW, Vrijman V, Al-Saady R, van der Meulen IJ, Mourits MP, Lapid-Gortzak R. Autorefraction versus subjective refraction in a radially asymmetric multifocal intraocular lens. *Acta Ophthalmol* 2014; 92:764–768
- Bissen-Miyajima H, Minami K, Yoshino M, Nishimura M, Oki S. Autorefraction after implantation of diffractive multifocal intraocular lenses. *J Cataract Refract Surg* 2010; 36:553–556
- Muñoz G, Albarrán-Diego C, Sakla HF. Autorefraction after multifocal IOLs. *Ophthalmology* 2007; 114:2100
- Goes FJ. Visual results following implantation of a refractive multifocal IOL in one eye and a diffractive multifocal IOL in the contralateral eye. *J Refract Surg* 2008; 24:300–305
- Gatinel D, Pagnoulle C, Houbrechts Y, Gobin L. Design and qualification of a diffractive trifocal optical profile for intraocular lenses. *J Cataract Refract Surg* 2011; 37:2060–2067
- Pesudovs K, Weisinger HS. A comparison of autorefractor performance. *Optom Vis Sci* 2004; 81:554–558
- Ogbuehi KC, Almaliki WH, AlQarni A, Osuagwu UL. Reliability and reproducibility of a handheld videorefractor. *Optom Vis Sci* 2015; 92:632–641
- Wang X, Dong J, Wu Q. Comparison of anterior corneal curvature measurements using a Galilei dual Scheimpflug analyzer and Topcon auto kerato-refractometer. *J Ophthalmol* 2014; 2014:140628
- McGinnigle S, Naroo SA, Eperjesi F. Evaluation of the auto-refraction function of the Nidek OPD-Scan III. *Clin Exp Optom* 2014; 97:160–163
- Micó V, Albarrán-Diego C, Thibos L. Power vectors for the management of astigmatism: from theoretical to clinical applications. In: Buckley R, ed. *Astigmatism: Types, Diagnosis and Treatment Options*. Hauppauge, NY, Nova Science Publishers, Inc., 2014; ISBN 10: 163321978X ISBN 13: 9781633219786
- Muñoz G, Albarrán-Diego C, Ferrer-Blasco T, García-Lázaro S. Power vector analysis as an aid to correct a rotated Artiflex toric phakic intraocular lens. *J Emmetropia* 2010; 1:213–217
- Campbell CE. Determining spherocylindrical correction using four different wavefront error analysis methods: comparison to manifest refraction. *J Refract Surg* 2010; 26:881–890
- McAlinden C, Khadka J, Pesudovs K. Statistical methods for conducting agreement (comparison of clinical tests) and precision (repeatability or reproducibility) studies in optometry and ophthalmology. *Ophthalmic Physiol Opt* 2011; 31:330–338
- Kretz FT, Linz K, Mueller M, Gerl M, Koss MJ, Gerl RH, Auffarth GU. Richtiges Refraktieren nach Implantation von Multifokal- und presbyopiekorrigierenden Intraokularlinsen [Refraction after Implantation of Multifocal and Presbyopia-Correcting Intraocular Lenses]. *Klinische Monatsblätter für Augenheilkunde* 2015; 232:953–956
- Albarrán-Diego C, Muñoz G, Ferrer-Blasco T. Subjective refraction before LASIK enhancement in biopsies procedures with refractive multifocal intraocular lenses. *J Refract Surg* 2011; 27:556–557
- Muñoz G, Albarrán-Diego C, Sakla HF. Validity of autorefraction after cataract surgery with multifocal ReZoom intraocular lens implantation. *J Cataract Refract Surg* 2007; 33:1573–1578
- Charman WN, Montés-Micó R, Radhakrishnan H. Problems in the measurement of wavefront aberration for eyes implanted with diffractive bifocal and multifocal intraocular lenses. *J Refract Surg* 2008; 24:280–286
- Campbell CE. Wavefront measurements of diffractive and refractive multifocal intraocular lenses in an artificial eye. *J Refract Surg* 2008; 24:308–311
- Jendritza BB, Knorz MC, Morton S. Wavefront-guided excimer laser vision correction after multifocal IOL implantation. *J Refract Surg* 2008; 24:274–279
- Siedlecki D, Ginis HS. On the longitudinal chromatic aberration of the intraocular lenses. *Optom Vis Sci* 2007; 84:984–989
- Varón C, Gil MA, Alba-Bueno F, Cardona G, Vega F, Millán MS, Buil JA. Stereo-acuity in patients implanted with multifocal intraocular lenses: is the choice of stereotest relevant? *Curr Eye Res* 2014; 39:711–719
- Charman WN, Jennings JA. Objective measurements of the longitudinal chromatic aberration of the human eye. *Vision Res* 1976; 16:999–1005
- Strang NC, Gray LS, Winn B, Pugh JR. Clinical evaluation of patient tolerance to autorefractor prescriptions. *Clin Exp Optom* 1998; 8:112–118
- Delori FC, Pflibsen KP. Spectral reflectance of the human ocular fundus. *Appl Opt* 1989; 28:1061–1077
- He JC, Marcos S, Burns SA. Comparison of cone directionality determined by psychophysical and reflectometric techniques. *J Opt Soc Am A Opt Image Sci Vis* 1999; 16:2363–2369
- Martin J, Vasudevan B, Himebaugh N, Bradley A, Thibos L. Unbiased estimation of refractive state of aberrated eyes. *Vision Res* 2011; 51:1932–1940
- Teel DF, Jacobs RJ, Copland J, Neal DR, Thibos LN. Differences between wavefront and subjective refraction for infrared light. *Optom Vis Sci* 2014; 91:1158–1166
- Vega F, Millán MS, Vila-Terricabras N, Alba-Bueno F. Visible versus near-infrared optical performance of diffractive multifocal intraocular lenses. *Invest Ophthalmol Vis Sci* 2015; 56:7345–7351
- Schwiegerling J, DeHoog E. Problems testing diffractive intraocular lenses with Shack-Hartmann sensors. *Appl Opt* 2010; 49:D62–D68
- Mojzis P, Peña-García P, Liehneova I, Ziak P, Alió JL. Outcomes of a new diffractive trifocal intraocular lens. *J Cataract Refract Surg* 2014; 40:60–69
- Toto L, Carpineto P, Falconio G, Agnifili L, Di Nicola M, Mastropasqua A, Mastropasqua L. Comparative study of Acrysof ReSTOR multifocal intraocular lenses + 4.00 D and + 3.00 D: visual performance and wavefront error. *Clin Exp Optom* 2013; 96:295–302

Disclosures: None of the authors has a financial or proprietary interest in any material or methods mentioned.